ELSEVIER

Development and characterization of new insulin containing polysaccharide nanoparticles

Bruno Sarmento [a,*], António Ribeiro [b], Francisco Veiga [c], Domingos Ferreira [a]

[a] Department of Pharmaceutical Technology, Faculty of Pharmacy of the University of Porto,
Rua Aníbal Cunha 164, 4050-030 Porto, Portugal
[b] Department of Pharmaceutical Technology, ISCSN, Gandra, Portugal
[c] Department of Pharmaceutical Technology, Faculty of Pharmacy of the University of Coimbra, Coimbra, Portugal

Abstract

A nanoparticle insulin delivery system was prepared by complexation of dextran sulfate and chitosan in aqueous solution. Parameters of the formulation such as the final mass of polysaccharides, the mass ratio of the two polysaccharides, pH of polysaccharides solution, and insulin theorical loading were identified as the modulating factors of nanoparticle physical properties. Particles with a mean diameter of 500 nm and a zeta potential of approximately -15 mV were produced under optimal conditions of DS:chitosan mass ratio of 1.5:1 at pH 4.8. Nanoparticles showed spherical shape, uniform size and good shelf-life stability. Polysaccharides complexation was confirmed by differential scanning calorimetry and Fourier transformed infra-red spectroscopy. An association efficiency of 85% was obtained. Insulin release at pH below 5.2 was almost prevented up to 24 h and at pH 6.8 the release was characterized by a controlled profile. This suggests that release of insulin is ruled by a dissociation mechanism and DS/chitosan nanoparticles are pH-sensitive delivery systems. Furthermore, the released insulin entirely maintained its immunogenic bioactivity evaluated by ELISA, confirming that this new formulation shows promising properties towards the development of an oral delivery system for insulin.

1. Introduction

Colloidal carriers made under mild conditions by complexation of oppositely charged natural polymers, also known as polyelectrolytes, represent a promising vehicle to protect proteins against harsh gastrointestinal conditions and to control the release rate of proteins [1–3]. Also, natural polysaccharides have demanded particular interest due to their attractive biocompatible, biodegradable, hydrophilic and protecting properties, which have demonstrated favourable characteristics for drug entrapment and delivery [4]. However, due to the labile physicochemical properties of proteins, gentle nanoencapsulation conditions must be provided to assure the maintenance of their structural bioactivity. Particular attention has been given to protein-loaded chitosan-based nanoparticles [5–7]. Chitosan,

an unbranched polyamine of D-glucosamine and *N*-acetyl glucosamine molecules, is characterized for its biodegradable, non-toxic and biocompatible properties [8] providing several biomedical, pharmaceutical and food applications. Moreover, chitosan has the significant potential of reducing transepithelial electrical resistance and transiently opening tight conjunction between epithelial cells [9]. In addition, its mucoadhesive property [10] is another advantage for promoting drug adsorption due to combination with anionic substructures such as sialic acid moieties of the mucosa layer. The adhesion of chitosan at the site of drug absorption offers various advantages for an improved uptake of therapeutic peptides [11,12].

Additional coincorporation of highly charged density polyanions onto chitosan nanoparticles can improve nanoparticle properties concerning protein association efficiency and modulation of drug release [13,14]. It has been previously noted that the stronger the protein–polyions complex is the slower will be the rate of protein release due to enhance of electrostatic interactions [15].

---

* Corresponding author. Tel.: +351 222078949; fax: +351 222003977.
  E-mail address: bruno.sarmento@ff.up.pt (B. Sarmento).

Taking into account these considerations, dextran sulfate (DS), a biodegradable and biocompatible branched negatively charged polyion with approximately 2.3 sulfate groups per glucosyl residue, was selected to formulate DS/chitosan nanoparticles. Chitosan and DS have been formulated as polyelectrolyte complex gels with swelling characteristics [16] and controlled release properties [17] and have been extensively used as multilayer films for cell culture [18]. Additionally, they are intrinsically hydrophilic, which contributes for longer circulation times *in vivo* and allows the encapsulation of water-soluble proteins.

In the present work insulin was chosen as the model protein. It is a well known 51 amino acids protein, produced nowadays by DNA recombination techniques and used subcutaneously in the treatment of diabetes *mellitus*. Although several attempts have been developed regarding alternative routes of insulin administration [19–21], the oral approach remains the most attractive due to convenience and high patient compliance. However, the bioavailability of insulin after oral administration is normally low, due to its low stability in the gastrointestinal tract (GI), low partition coefficient and the physical barrier of the intestinal epithelium. One approach to improve the gastrointestinal uptake of low molecular weight proteins is to bind them to colloidal systems like nanoparticles, protecting them from degradation in the gastrointestinal tract and promoting the transport into systemic circulation [22,23].

Since the size of nanoparticles and protein stability are essential for an efficient pharmacologic effect of insulin, the main objective of this paper was to establish a nanoparticulate system produced by polyelectrolyte complexation between DS and chitosan, and evaluate their potential as insulin carriers. The physical and morphological properties of nanoparticles were investigated in accordance with formulation parameters and the release profile of insulin was also determined regarding its potential for oral delivery.

2. Materials and methods

2.1. Materials

Low molecular weight (MW) chitosan ($\approx$50 kDa) and low MW dextran sulfate (8 kDa) were purchased from Sigma (Portugal). High MW dextran sulfate (500 kDa) was obtained from PKC® (Denmark). Dextran sulfate stock solutions were prepared in deionized water (Milli-Q®) by overnight magnetic stirring and chitosan solutions were prepared by dissolution of chitosan in deionized water containing 1% (v/v) acetic acid followed by filtration through a paper filter Millipore #2 and stored at 4 °C. Human zinc-insulin crystal (Lot RS0325, 7.0 mg lyophilized human biosynthetic insulin per vial) was a gift from Lilly Portugal.

2.2. Preparation of nanoparticles

Nanoparticle complexation between DS and chitosan was performed employing aqueous solutions of oppositely charged polymers in a final volume of 120 mL. Unless otherwise mentioned, complexes were obtained after dropwise addition of chitosan solution at pH 5.0 to DS solution at pH 3.2 under magnetic stirring followed by additional mixing for 15 min at 600 rpm to final concentrations of 0.15% DS and 0.10% chitosan (DS/chitosan mass ratio 1.5:1). For insulin association, 7 mg of the protein was previously dissolved in the DS solution before chitosan complexation. These conditions were obtained after preliminary studies that provided the best results taking into account the desired mean particle size and insulin association efficiency.

2.3. Nanoparticle characterization

Measurements of particle size were performed by photon correlation spectroscopy (PCS) at 25 °C with a detection angle of 90° and zeta potential by laser Doppler anemometry (LDA) using a Malvern Zetasizer and Particle Analyzer 5000 (Malvern Instruments) ($n \geq 6$).

2.4. Stability of nanoparticles

The stability of nanoparticles was determined monitorizing their mean particle size and zeta potential over time. After production, nanoparticles were stored at 4 °C in aqueous solution and then the size and zeta potential were measured after 0, 7, 14, 28, 42 and 60 days of shelf-life.

2.5. Isolation of particles

Nanoparticles were collected by centrifugation at 14,000 rpm (20,000 × g) for 45 min. Supernatant were used for insulin determination. Nanoparticles were kept at 4 °C for further experiments.

2.6. Insulin association efficiency

The amount of insulin associated with the particles was calculated by the difference between the total amount used to prepare the particles and the amount of insulin present in the aqueous phase after centrifugation. The association efficiency (AE) was determined indirectly applying the following equation:

$$AE = \frac{\text{total amount of insulin} - \text{free insulin in supernatant}}{\text{total amount of insulin}} \times 100$$

2.7. In vitro release studies

Nanoparticles were placed into 20 mL of USP XXVI buffers, namely hydrochloric acid pH 1.2, acetate pH 4.5, acetate pH 5.2 and phosphate pH 6.8 and incubated at 37 °C under magnetic stirring. At pre-determined time intervals, samples were taken for insulin determination and replaced by fresh medium.

2.8. Insulin determination

Insulin concentration was determined spectrophotometrically using the Coomassie PlusTM Bradford Assay (Pierce,

Rockford, USA) modified Bradford assay [24]. Briefly, insulin samples and Bradford reagent were mixed at 1:1 (v/v) ratio in a 96-well plate and incubated at room temperature for 15 min. The absorbance was measured at 595 nm on a thermomax plate reader (PowerWaveX; Bio-Tek, Winooski, VT, USA). Calibration curves were made using supernatant of unloaded particles for AE and unloaded nanoparticles for *in vitro* release profile. All the results were made in triplicate.

2.9. Scanning (SEM) and transmission (TEM) electronic microscopy

For the SEM analysis, nanoparticles were mounted on metal stubs using adhesive tape, gold coated under vacuum and examined on a JEOL JSM-840 SEM (Japan). For TEM, one drop of sample was placed in a grid, treated with uranil acetate and observed in a Zeiss EM 902A TEM.

2.10. Differential Scanning calorimetry (DSC)

Thermograms were obtained using a Shimadzu DSC-50 system (Shimadzu, Kyoto, Japan). Samples were lyophilized, crimped in a standard aluminium pan and heated from 20 to 350 °C at a rate of 10 °C/min under constant purging of nitrogen at 20 ml/min.

2.11. Fourier transform infra-red (FTIR) analysis

IR-spectra were measured using a Bomem IR-spectrometer (Bomem, Canada). Samples were lyophilized, gently mixed with 300 mg of micronized KBr powder and compressed into discs at a force of 10 kN for 2 min using a manual tablet presser (Perkin Elmer, Norwalk, USA). For each spectrum a 256-scan interferogram was collected with a 4 cm^{-1} resolution in the mid-IR region at room temperature. Insulin spectra were obtained according to a double subtraction procedure [25] and insulin-free systems and water vapor spectra were collected under identical conditions for blank subtraction. All samples were run in triplicate and the data shows the average of the three measurements.

2.12. Immunological bioactivity of insulin

The integrity of the insulin released from nanoparticles was assessed by a reported HPLC method [26] while its bioactivity was assayed by an ELISA test (Mercodia, Uppsala, Sweden). Aliquots of samples taken during release assays were accu-

rately diluted with deionized water (Milli-Q®) regarding the ideal concentration range of the method (1–200 mU/l) using the manufacture's protocol and its relative bioactivity was calculated by comparison with values obtained by Bradford analysis of the same aliquots.

2.13. Statistical analysis

The *t*-test and the one-way analysis of variance (ANOVA) with the pairwise multiple comparison procedures (Student–Newman–Keuls method) were performed to compare two or multiple groups, respectively. All analyses were run using the SPSS program (Version 14.0, SPSS Inc., USA) and differences were considered to be significant at a level of $P < 0.05$.

3. Results and discussion

Complex coacervation between chitosan and DS is a mild process and was used to prepare nanoparticles at ambient temperature without using sonication or organic solvents. Resulting DS/chitosan nanoparticle colloidal suspension presented a deep and typical Tyndall effect. Thus, it is a suitable procedure to encapsulate sensitive materials such as proteins, which are sensitive to different stress factors [27]. Being insulin an amphoteric molecule it is able to be electrostatically attached to such nanoparticles composed of DS and chitosan with a high avidity, allowing its association with the stable colloidal drug carrier. The insulin monomer contains many ionizable groups due to 6 amino acid residues capable of attaining a positive charged polyelectrolyte like chitosan and 10 amino acid residues capable of attaching a negative charged polyelectrolyte like DS [28]. These properties might be highly responsible for the entrapment of insulin into DS/chitosan nanoparticles.

Factors affecting the characteristics of DS/chitosan nanoparticles and the optimal conditions for their preparation were studied.

Primary assays were done in order to establish the range of polyelectrolytes concentration to produce nanoparticles with an appropriate submicron size and a significant value of insulin AE. Therefore, concentrations range from 0.05% to 0.20% for both chitosan and DS were used to prepare nanoparticles in the proportion of 1:1, at final pH of 4.8. Results are depicted in Table 1.

As expected, increasing the polyelectrolytes concentration led to an increase of nanoparticles mean size in a linear dependency.

Table 1
Influence of polyelectrolytes concentration on nanoparticle properties

DS (%)	Chitosan (%)	*z*-Average number (nm)	AE (%)	Zeta potential (mV)
0.05	0.05	479 ± 118[*]	54.7 ± 4.8[*]	0.2 ± 0.1
0.10	0.10	665 ± 210	71.5 ± 2.9[*]	−0.4 ± 0.1
0.15	0.15	846 ± 100	87.4 ± 2.7[*]	1.2 ± 0.3
0.20	0.20	1012 ± 187[*]	96.4 ± 4.3[*]	3.2 ± 0.4

The ratio between chitosan and DS was kept at 1/1 (w/w).
[*] The mean difference is significant at the 0.05 level.

Table 2
Influence of DS:chitosan mass ratio on nanoparticle properties

DS (%)	Chitosan (%)	DS:chitosan mass ratio	z-Average number (nm)	AE (%)	Zeta potential (mV)
0.05	0.10	1:2	1612 ± 248[*]	48.6 ± 7.7[*]	2.4 ± 0.1[*]
0.10	0.10	1:1	665 ± 210	71.5 ± 2.9[*]	−0.4 ± 0.1[*]
0.15	0.10	1.5:1	489 ± 11	85.4 ± 0.5	−14.2 ± 0.5[*]
0.20	0.10	2:1	598 ± 25	87.2 ± 0.9	−16.7 ± 0.9[*]
0.25	0.10	2.5:1	619 ± 39	90.6 ± 1.2	−21.5 ± 1.6[*]

[*] The mean difference is significant at the 0.05 level.

Zeta potential was near zero for all formulations, which indicates that the balance between positive and negative charges is similar, as expected from positive and negative mass of both polyelectrolytes.

The AE of insulin was also directly related to the polyelectrolytes concentration. This trend is in agreement with the mechanism of protein association to polyelectrolyte nanoparticles mediated by ionic interactions. The presence of higher concentrations of polyelectrolytes probably shifts the ionic equilibrium between insulin and polyelectrolytes towards the associated complexes. Similar conclusion was also drawn from insulin-loaded chitosan/TPP nanoparticles [29].

Considering the desired nanoscale size and insulin AE, 0.10% chitosan concentration was chosen for further experiments. Then, attempts to find the best DS:chitosan mass ratio were done according stoichiometries shown in Table 2.

Nanoparticles formulated with a DS:chitosan mass ratio of 1:2 showed a higher mean particle size than obtained with a polysaccharides ratio of 1:1, 1.5:1, 2:1 and 2.5:1 ($P < 0.05$), but no significant differences were found between these last three mass ratios. The finding that the ideal DS:chitosan mass ratio is higher than 1:1 indicates that DS is possibly a colloidal protector preventing particle aggregation and simultaneously a robustness factor of nanoparticles strength. In fact, only chitosan shows gelling properties. DS does not swells in aqueous environment, probably inducing a squeeze effect on the nanoparticle matrix by increasing the final DS:chitosan mass ratio.

Zeta potential of the systems was dependent on the polyelectrolytes ratio. The zeta potential was almost zero for a DS:chitosan mass ratio of 1:1, but decreased to −14.2 mV when more negative charged DS was added (1.5:1) and even more (−16.7) when that ratio reached 2:1. Thus, one can deduce that the excess of DS is placed mainly on the surface of the nanoparticle, which may interact with positively charged insulin and therefore increase of insulin AE.

The obtained values for insulin AE showed a DS:chitosan mass ratio dependency. The increase in DS/chitosan ratio from 1:2 to 1.5:1 allowed the entrapment of more insulin although higher mass ratio than 1.5:1 did not originate any variation on insulin AE ($P > 0.05$). It can be postulated that the affinity of insulin to sulfate groups of DS is higher than for amine groups of chitosan due the stronger electrostatic interaction between positively charged protein and negative sulfate groups. Thus, the DS:chitosan mass ratio of 1.5:1 appeared to be adequate to entrap a higher amount of insulin. Nanoparticles formulated with a DS:chitosan mass ratio of 1.5:1 (0.15% DS and 0.1% chitosan) was then selected to analyze the effect of additional curing on nanoparticles properties. In order to assess this parameter, nanoparticles were produced and additionally stirred for 5, 15 and 30 min. The obtained results are summarized in Table 3.

The effect of nanoparticles curing time did not show any statistical differences on the nanoparticles mean size ($P > 0.05$), which suggests a fast complexation between polyelectrolytes and a stabilization effect during additional stirring. The decrease of zeta potential with the curing time can be explained by the surface attachment of additional negative DS molecules in excess in the surrounding aqueous medium, which is accompanied by a slight increase of particle mean size. Furthermore, insulin AE was independent on additional curing time since obtained results for different curing times were statistically similar ($P > 0.05$). One can assume that insulin interaction with polyelectrolytes happens very fast remaining the protein entrapped within the nanoparticles.

Then, nanoparticles were produced with a different MW DS. Nanoparticles produced with both 8 and 500 kDa MW DS originated practically the same mean particle size around 490 nm and zeta potential around −15 mV, but the decrease of DS MW from 500 to 8 kDa originated a small decrease of insulin AE from 85.4 to 81.4% ($P < 0.05$). Apparently, a longer polyanion chain has the capacity to bind proteins in a stronger complex [15]. DS is probably the major responsible for the association of insulin to nanoparticles and therefore its MW can be important to determine the degree of association to insulin.

The effect of theorical insulin loading was investigated by varying the final polymer:insulin mass ratio to produce different nanoparticles and the results are depicted in Table 4.

Table 3
Influence of curing time on nanoparticle properties

DS (%)	Chitosan (%)	Time of curing (min)	z-Average number (nm)	AE (%)	Zeta potential (mV)
0.15	0.10	5	452 ± 45	84.3 ± 1.5	−9.3 ± 0.3[*]
0.15	0.10	15	489 ± 11	85.4 ± 0.5	−14.2 ± 0.5[*]
0.15	0.10	30	543 ± 76	85.2 ± 2.0	−17.0 ± 0.3[*]

[*] The mean difference is significant at the 0.05 level.

Table 4
Influence of polymer:insulin mass ratio on nanoparticle properties

DS (%)	Chitosan (%)	Theorical insulin (%)	z-Average number (nm)	AE (%)	Zeta potential (mV)
0.15	0.10	0	493 ± 86	–	−16.4 ± 2.6
0.15	0.10	0.0012	504 ± 53	86.7 ± 1.9	−18.9 ± 0.5
0.15	0.10	0.0035	527 ± 44	84.2 ± 0.8	−15.7 ± 0.1
0.15	0.10	0.007	489 ± 11	85.4 ± 0.5	−14.2 ± 0.5
0.15	0.10	0.01	603 ± 26	87.3 ± 1.9	−10.5 ± 0.1[*]

[*] The mean difference is significant at the 0.05 level.

Table 5
Influence of pH of chitosan solution on nanoparticle properties

DS pH	Chitosan pH	Final pH	z-Average number (nm)	AE (%)	Zeta potential (mV)
3.25	5.0	4.8	489 ± 11	85.4 ± 0.5[*]	−14.2 ± 0.5
3.25	4.0	3.9	505 ± 8	90.8 ± 1.3	−8.9 ± 0.5[*]
3.25	3.0	3.2	522 ± 19	93.0 ± 1.5	−5.7 ± 0.1[*]

[*] The mean difference is significant at the 0.05 level.

Mean particle size was found to be statistically independent on the theorical insulin loading as well as the insulin AE. In the range of initial insulin concentration studied, the theorical insulin loading capacity varied from 0.5% to 3.8% (w/w). These values are relative low to expect a significant effect of insulin concentration on the final nanoparticle properties, as observed. Therefore, the capacity of saturation of nanoparticles with insulin seems not to be reached in this insulin concentration range and, consequently, the ionic nature of insulin association to nanoparticles is highlighted here. Zeta potential of nanoparticles slightly decreased with increasing theorical insulin loading, clearly indicating that a significant fraction of the protein is attached to the surface of the nanoparticles.

Because of the acidic properties of DS ($pK_a < 1$), it probably shows negative sulfate groups in a wild range of pH. Chitosan as an ionizable polymer contains different properties according the pH environment where it is dissolved. Consequently, nanoparticles properties are probably dependent on the pH of aqueous solution where they are produced. To assess this hypothesis, different nanoparticles where formulated, varying the final pH of colloidal system by using chitosan dropping solutions at different pH (Table 5).

The variation of the final pH of nanoparticles production between 4.8 and 3.2 did not significantly influence their mean particle size. However, it decreased the value of zeta potential, probably because the degree of ionization of DS shifts towards its protonated form. Insulin AE increased with the decrease of the final pH from 4.8 to 3.2 mostly because insulin must be highly protonated at lower pH and, probably, the alteration of ionizable state of the protein promotes its interaction with sulfate groups of DS.

The stability of nanoparticles was determined by the variation of their mean particle size and zeta potential with the time. After production, nanoparticles were stored at 4 °C in aqueous environment and at pre-determined times, size an zeta potential were measured as described before. Table 6 shows the values found.

The results did not show significant differences on nanoparticles mean size and zeta potential up to 28 days of storage. An increasing effect was observed on size and zeta potential, after 28 and 42 days, respectively. This effect may be attributed to some aggregation of nanoparticles.

The morphology of DS/chitosan nanoparticles is depicted in Figs. 1 and 2. SEM micrograph of DS/chitosan nanoparticles (Fig. 1) shows clustered spherical-like particles, with smooth surfaces. Nevertheless, they were easily resuspended in aqueous solution. Also, they showed a broad uniform size, in agreement with photon spectroscopy analysis (Table 2).

TEM images revealed well-defined spherical nanoparticles. Inner dark color is probably due to a deposition of the stain suggesting a relatively high density of nanoparticles matrix. Also, it is visible the superficial deposition of DS on the nanoparticles produced with an excess of DS on the final formulation, which confirms the hypothesis that DS is a colloidal protector preventing particle aggregation.

The thermograms of DS/chitosan nanoparticles and isolated polyelectrolytes are depicted in Figs. 3–5. The DS/chitosan nanoparticles exhibited a DSC broad endothermic peak between 50 and 110 °C and an exothermic peak at 222.5 °C, an intermediated value of the endothermic peaks obtained for isolated polyelectrolytes. Isolated polymers were characterized by the presence of initial endothermic peaks at 62.0 and 60.6 °C for

Table 6
Influence of storing time on mean diameter and zeta potential of nanoparticle's produced with a DS:chitosan mass ratio of 1.5:1

Time (days)	z-Number (nm)	Zeta potential (mV)
0	538 ± 22	−14.2 ± 0.5
7	534 ± 21	−11.1 ± 0.9
14	589 ± 58	−12.1 ± 1.1
28	623 ± 72	−9.3 ± 1.1[*]
42	678 ± 15[*]	−9.0 ± 3.6[*]
60	754 ± 20[*]	−3.2 ± 1.9[*]

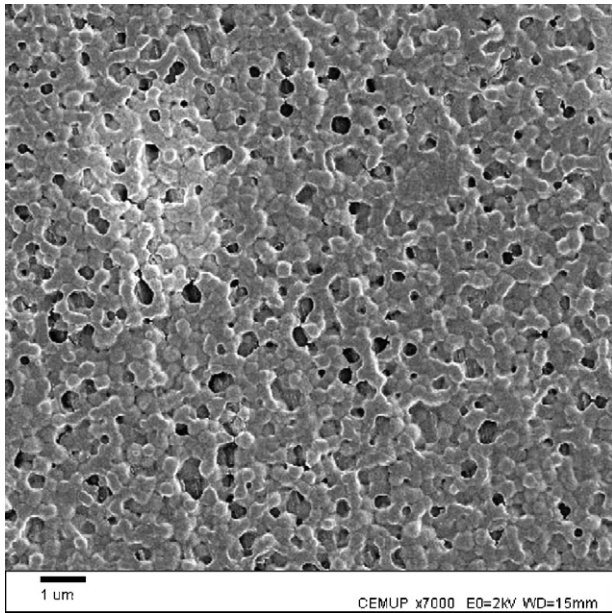[*] The mean difference is significant at the 0.05 level.

Fig. 1. SEM micrographs of DS/chitosan nanoparticles produced with a DS:chitosan mass ratio of 1.5:1 at pH 4.8.
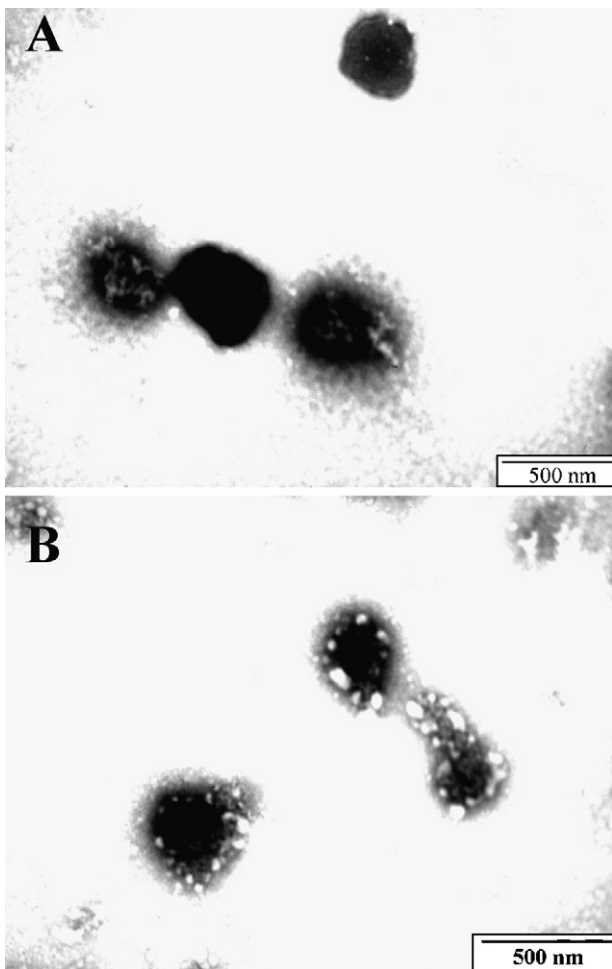

Fig. 2. TEM micrographs of DS/chitosan nanoparticles produced with a DS:chitosan mass ratio and of 1.5:1 (A) and 2:1 (B), both systems at pH 4.8.
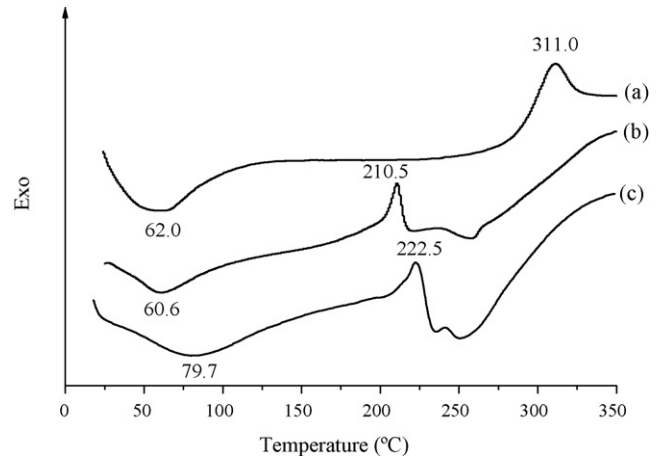

Fig. 3. Thermograms of (a) chitosan at pH 5.0, (b) dextran sulfate at pH 3.25 and (c) DS/chitosan nanoparticles produced with a DS:chitosan mass ratio of 1.5:1 at final pH of 4.8.
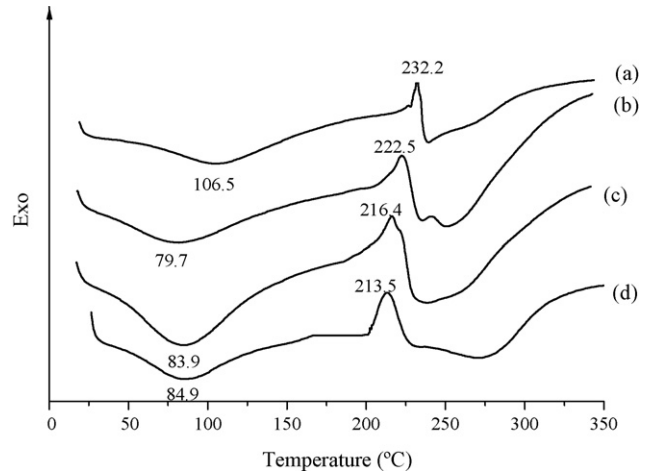

Fig. 4. Thermograms of DS/chitosan nanoparticles produced with a DS:chitosan mass ratio of (a) 1:1, (b) 1.5:1, (c) 2:1 and (d) 2.5:1.
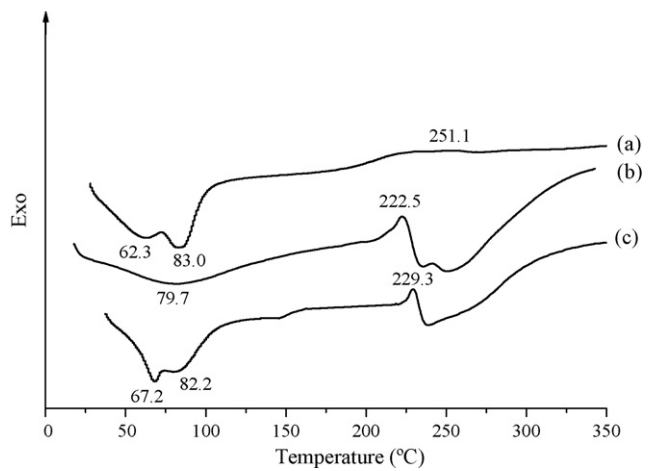
Fig. 5. Thermograms of (a) insulin, (b) empty DS/chitosan nanoparticles and (c) insulin-loaded DS/chitosan nanoparticles produced with a DS:chitosan mass ratio of 1.5:1 at pH of 4.8.

chitosan and DS, respectively, and higher exothermic peaks at 311.0 and 210.5 °C, respectively (Fig. 3). Endothermic peaks have been correlated with evaporation of water associated to hydrophilic groups of polymers while exothermic peaks have been related to degradation of polyelectrolytes due to dehydration, depolymerization and pyrolitic reactions [30,31].

The exothermic peak of DS/chitosan nanoparticle is interpreted as the cleavage of electrostatic interactions between both polyelectrolytes. Similar electrostatic interactions have been referred to explain chitosan/DS interactions [17,32]. Additional exothermic behaviour was observed for temperatures higher than 325 °C, which is probably evidence of polymer decomposition. When comparing the temperature of water evaporation in isolated polymers and nanoparticles, one can found that it occurred later on nanoparticle thermogram. Probably, a tiny amount of water remained associated in the nanoparticle matrix to hydrophilic residues of polymers and required higher temperature to be completely removed. This hypothesis strongly supports the assumption of the formation of a high nanoparticle matrix density.

Analyzing the effect of DS:chitosan mass ratio on the thermograms of different nanoparticles (Fig. 4), it is noted that by increasing this ratio, the value of the exothermic peak, firstly attributed to the cleavage of electrostatic interactions between both polyelectrolytes decreases, approaching to the exothermic peak of isolated DS (210.5 °C). This can be assumed that the contribution of DS mass to the overall nanoparticles mass is as higher as the initial DS:chitosan mass ratio. Thus, the higher is the overall DS mass, the lower is the relative number of negative charge groups that contribute to the electrostatic interaction with positive chitosan, decreasing the amount of energy required for the cleavage of electrostatic interactions It can also be confirmed by the lower value of the exothermic peak observed for higher DS:chitosan mass ratio nanoparticles.

The thermogram of pure insulin shows two endothermic peaks at 62.3 and 83.0 °C and a tiny and broad exothermic peak at 251.1 °C (Fig. 5). The two endothermic peaks attributed to denaturation process and water loss [33] continued appearing on the insulin-loaded nanoparticles, indicating not only that it was successfully entrapped but also that no significant damage might have occurred in insulin structure. First endothermic peak seems to be a contribution of insulin, chitosan and DS and the second, of minor intensity, a transition associated with the protein. The exothermic peak registered at 229.3 °C appeared shifted to higher exothermic temperature than DS/chitosan nanoparticles, which can be understood by an interaction between nanoparticle components and a slight increase of resistance to thermic degradation. This resistance is probably the result of a new ionic chemical interaction between opposite group charges.

In order to confirm DS/chitosan interactions, isolated polyelectrolytes and nanoparticles were analyzed by FTIR spectroscopy. Fig. 6 shows spectra of DS, chitosan and DS/chitosan nanoparticles.

The FTIR spectrum of chitosan shows a peak of amide bond at 1636 cm^{-1} due to C=O stretching and C–N stretching vibration, a strong protonated amino peak at 1573 cm^{-1} from N–H bending and at 1411 cm^{-1} from N–H stretching
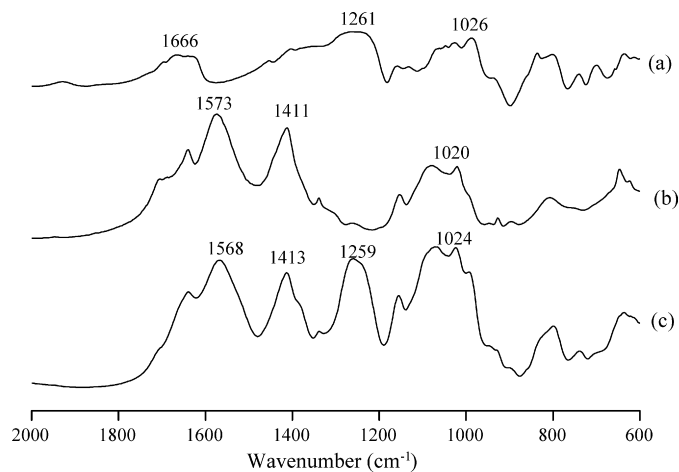
Fig. 6. FTIR spectra of (a) dextran sulfate at pH 3.25, (b) chitosan at pH 5.0 and (c) DS/chitosan nanoparticles produced with a DS:chitosan mass ratio of 1.5:1 at pH 4.8.

because it is obtained from partial *N*-deacetylation of chitin. In addition, the peak absorbance of amino groups of chitosan at 1153 cm^{-1} (N–H blending vibration) was also present as well as the peak around 1020 cm^{-1} originated by the symmetric stretch of C–O–C. DS presented sulfyl peaks near 1026 cm^{-1} (symmetric SOO$^-$ stretching vibration) and 1261 cm^{-1} (asymmetric SOO$^-$ stretching vibration) as well as a band around 820 cm^{-1} corresponding to S–O–S vibrations. Chitosan peak at 1411 cm^{-1} and DS peak at 1261 cm^{-1} can be used to monitorize the formation of nanoparticles since they are exclusive of both polymers. FTIR spectrum of DS/chitosan nanoparticles revealed small changes in the amine and sulfate absorption bands at 1568 and 1024 cm^{-1}, but peaks at 1413 and 1259 cm^{-1} were consistent with the presence of electrostatic interactions, clearly indicated the presence of both polyelectrolytes in the final nanoparticle composition.

Attempts to investigate the entrapment of insulin into DS/chitosan nanoparticles were also done through FTIR analysis. Fig. 7 depicts FTIR spectra of insulin, empty DS/Chitosan and insulin-loaded DS/chitosan nanoparticles.
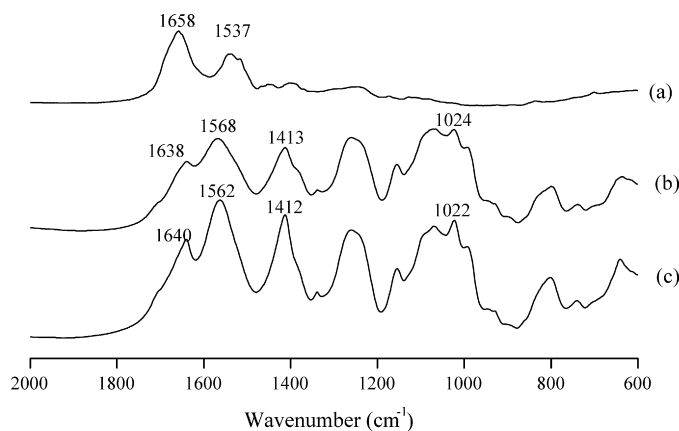
Fig. 7. FTIR spectra of (a) insulin, (b) DS/chitosan nanoparticles and (c) insulin-loaded DS/chitosan nanoparticles produced with a DS:chitosan mass ratio of 1.5:1 at pH 4.8.
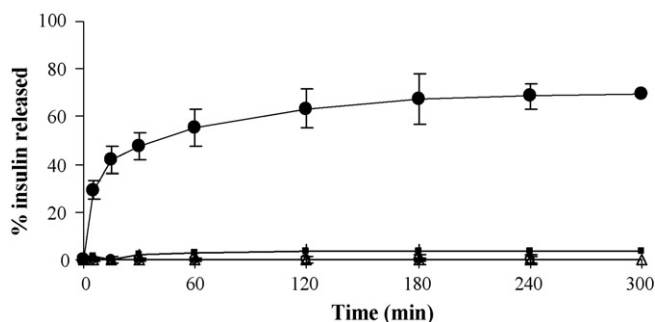
Fig. 8. Insulin cumulative release profile from insulin-loaded DS/chitosan nanoparticles produced with DS:chitosan mass ratio of 1.5:1 at final pH of 4.8. Nanoparticles were submitted to curing time of 15 min and the theorical insulin loading was 2.3% (final insulin 0.006%). Release assay was performed at pH 1.2 (△), 4.5 (○), 5.2 (■) and 6.8 (●) (vertical bars represent standard derivations based on three replicates).

Insulin spectrum reveals two peaks on the nanoparticle absorption bands in the Amide I ($\sim$1650 cm^{-1}) and Amide II ($\sim$1540 cm^{-1}) mainly due C=O stretching vibration, which is characteristic of protein spectrum. These two peaks are also present in the insulin-free DS/chitosan nanoparticle spectrum. Therefore, after insulin entrapment, nanoparticle spectrum presents a very similar aspect compared with insulin-unloaded nanoparticles. However, an increase of the peak intensity at 1562 cm^{-1} and mainly at 1640 cm^{-1} can be understood as the presence on insulin.

Insulin release behaviour from DS/chitosan nanoparticle was evaluated at different aqueous pH buffers. The results are plotted in Fig. 8.

No insulin released from nanoparticles placed at pH of 1.2 and 4.5 and 5.2, was detected whilst at pH 6.8 insulin release presented a sustained release profile with 40% of insulin being released within the first 15 min following a lower release rate. After 300 min of the assay time, the amount of insulin released at pH 1.2 and 4.5 was insignificant and at pH 5.2, less than 4% of insulin was liberated. At pH lower than p*I* of insulin (5.3) [28], insulin presents an overall positive charge that is able to deeply interact with the polyanionic charge of nanoparticles provided by DS. At this pH range, the strong electrostatic interactions between insulin and DS may contribute to retain insulin in the DS/chitosan network. Additionally, DS/chitosan nanoparticles appear to preserve their physical integrity which also contributes to minimize insulin release by nanoparticle erosion. After 300 min of assay at pH 6.8, 70% of insulin was released and reached 73% after 24 h (Fig. 9). The initial stage of insulin release at pH 6.8 is attributed to the insulin located at the surface of the nanoparticles and the remainder of the unreleased insulin is most probably entrapped within the nanoparticles. These results lead to assume that the *in vitro* release behaviour of insulin from DS/chitosan nanoparticles was according to a dissociation mechanism and DS/chitosan nanoparticles are pH-sensitive delivery systems.

Fig. 9 represents the cumulative release profile of insulin from different DS/chitosan nanoparticles produced at different pH environment. It can be observed that the release rate was dependent on the pH of nanoparticle formation. Insulin
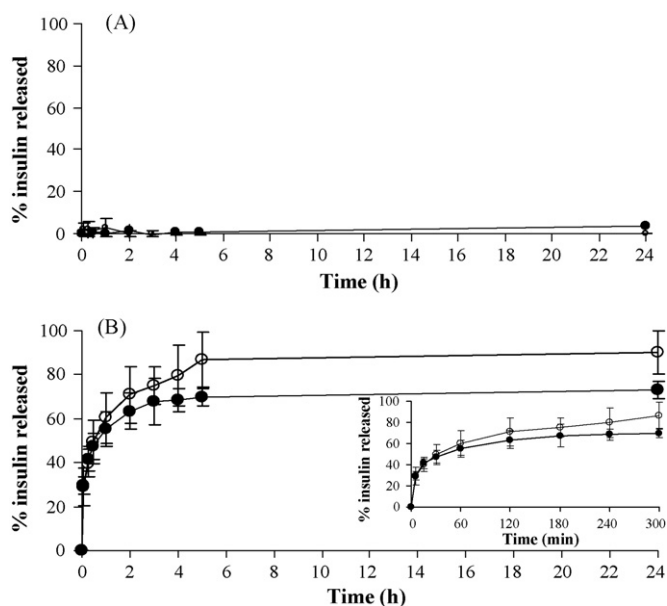

Fig. 9. Insulin cumulative release profile at pH 1.2 (A) and 6.8 (B) from insulin-loaded DS/chitosan nanoparticles prepared at pH 4.8 (close symbols) and 3.2 (open symbols) (vertical bars represent standard derivations based on three replicates).

release from nanoparticles produced at pH 3.2, with a higher insulin AE value, was faster than nanoparticles produced at pH 4.8. Nanoparticles prepared at higher pH may have produced stronger insulin–polyelectrolytes interactions, even though it might have occurred in a lower degree.

The effect of DS:chitosan mass ratio on the insulin cumulative release at pH 6.8 was then studied. As outlined in Fig. 10, the increase of DS:chitosan mass ratio from 1:1 to 2:1 decreased the insulin cumulative release. After a 24 h-assay insulin release from nanoparticles prepared with DS:chitosan mass ratio of 1:1, 1.5:1 and 2:1 was 76%, 73% and 59%, respectively. This finding suggested once more the main role of DS on insulin entrapment as well on the sustained effect of insulin release.

Most of the time, the pharmaceutical properties of therapeutic proteins closely depends on the retention of their biological activity. Consequently, the pharmaceutical efficacy should be assessed by monitoring the biological activity of protein at the
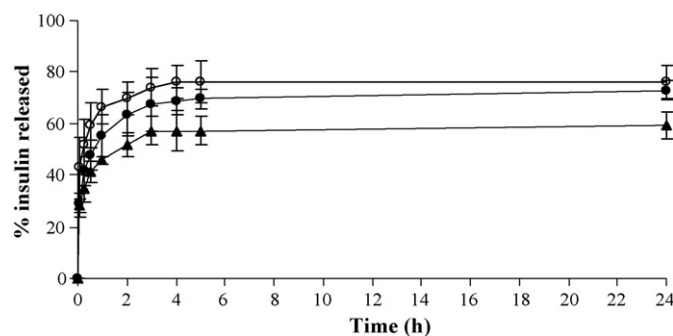

Fig. 10. Insulin cumulative release profile at pH 6.8 from insulin-loaded DS/chitosan nanoparticles produced with different a DS:chitosan mass ratio of 1:1 (○), 1.5:1 (●) and 2.0:1.0 (▲) (vertical bars represent standard derivations based on three replicates).
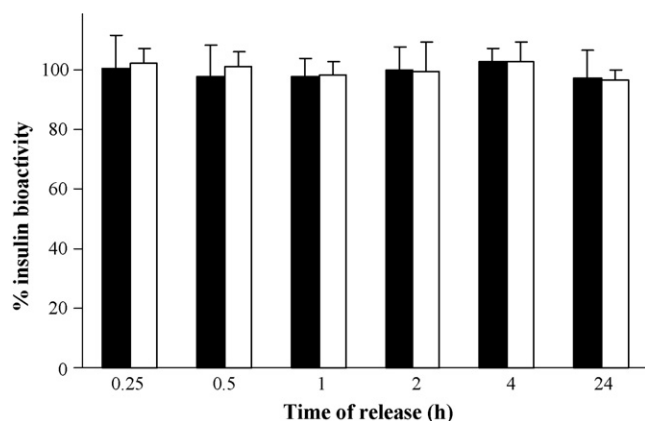
Fig. 11. The ELISA relative bioactivity of insulin released at pH 6.8 from DS/chitosan nanoparticles produced with a DS:chitosan mass ratio of 1.5:1 (black bars) and 2.1 (white bars) (results represent mean and standard deviation based on three replicates).

end of the formulation process [34]. To determine the relative immunogenic bioactivity of insulin, a specific solid phase two-site enzyme-linked immunosorbent assay (ELISA) was applied. Electrostatic as well as hydrophobic interactions play a role in the interaction between paratope of antibody and epitope of insulin and, thus, it is assumed that protein epitopes are to some extent conformation dependent [35]. Upon coating of ELISA plate with insulin, the possible loss of epitopes could be a consequence of insulin structural change. As shown in Fig. 11, the insulin released from nanoparticles in simulated intestinal pH without enzymes kept entirely its bioactivity for at least 24 h. These results seem to indicate that the insulin did not suffer any degradation process, namely hydrolyses or fibrillation instead maintained its active form.

Results obtained in preliminary HPLC assays showed a unique and well-defined peak on the chromatogram and no hydrolysis degradation products of insulin were detected (results not shown). Thus, insulin retained its primary structure after exposure to the intestinal 6.8 pH up to 24 h. The same conclusion was obtained when analyzing the residual insulin chromatogram released at pH 1.2, 4.5 and 5.2 where a single peak was detected (results not shown).

Regarding the insulin fibrillation process, the formation of insulin fibres from human insulin at simulated intestinal pH with a lag time of 49.4 h has been reported [36]. Also, at the concentration range of 0.05 mg/ml, the same obtained in the present work, insulin was described predominately in a dimer/hexamer form which is a factor of fibrillation delay [37]. Consequently, it is reasonable to assume that insulin molecules did not suffer fibrillation neither during nanoparticles production nor during the release time up to 24 h.

4. Conclusion

DS/chitosan nanoparticles produced by a mild coacervation method are suggested as a valid alternative to encapsulate insulin. Nanoparticles formulated by dropwise addition of a chitosan solution at pH 5 into a DS/insulin solution at pH 3.2 according to a DS:chitosan mass ratio of 1.5:1, followed by 15 min of curing time, were selected as the optimized formulation. Their morphology was assessed by electronic microscopy, confirming obtained granulometric analysis performed by photon correlation spectroscopy. The interaction between polyelectrolytes and insulin was successfully confirmed by DSC and FTIR. Release studies established the ability of these nanoparticles to retain insulin at simulated gastric medium and pH buffers of 4.5 and 5.2 values and a sustained release profile up to 24 h at simulated intestinal medium. Quantification of insulin released from nanoparticles by ELISA showed the preservation of its immunogenic bioactivity, which supports the application of these nanoparticles as oral delivery systems for insulin. Present investigations are being performed regarding the assessment of insulin *in vivo* oral bioactivity.

Acknowledgements

References

[1] W. Tiyaboonchai, J. Woiszwillo, R.C. Sims, C.R. Middaugh, Insulin containing polyethylenimine–dextran sulfate nanoparticles, Int. J. Pharm. 255 (2003) 139–151.

[2] S. Dumitriu, E. Chornet, Inclusion and release of proteins from polysaccharide-based polyion complexes, Adv. Drug Deliv. Rev. 31 (1998) 223–246.

[3] I. Lacik, A.V. Anilkumar, T.G. Wang, A two-step process for controlling the surface smoothness of polyelectrolyte-based microcapsules, J. Microencapsul. 18 (2001) 479–490.

[4] V.R. Sinha, R. Kumria, Polysaccharides in colon-specific drug delivery, Int. J. Pharm. 224 (2001) 19–38.

[5] O. Borges, G. Borchard, J.C. Verhoef, A.d. Sousa, H.E. Junginger, Preparation of coated nanoparticles for a new mucosal vaccine delivery system, Int. J. Pharm. 299 (2005) 155–166.

[6] Y. Chen, V.J. Mohanraj, J.E. Parkin, Chitosan–dextran sulfate nanoparticles for delivery of an anti-angiogenesis peptide, Lett. Pept. Sci. 10 (2004) 621–629.

[7] P. Calvo, C. Remunan-Lopez, J.L. Vila-Jato, M.J. Alonso, Chitosan and chitosan/ethylene oxide–propylene oxide block copolymer nanoparticles as novel carriers for proteins and vaccines, Pharm. Res. 14 (1997) 1431–1436.

[8] L. Ilium, Chitosan and its use as a pharmaceutical excipient, Pharm. Res. 15 (1998) 1326–1331.

[9] P. Artursson, Effect of chitosan on the permeability of monolayers of intestinal epithelial cells (Caco-2), Pharm. Res. 11 (1994) 1358–1361.

[10] C.-M. Lehr, J.A. Bouwstra, E.H. Schacht, H.E. Junginger, In vitro evaluation of mucoadhesive properties of chitosan and some other natural polymers, Int. J. Pharm. 78 (1992) 43–48.

[11] M. Thanou, J.C. Verhoef, H.E. Junginger, Chitosan and its derivatives as intestinal absorption enhancers, Adv. Drug Deliv. Rev. 50 (2001) 91–101.

[12] M. Thanou, J.C. Verhoef, H.E. Junginger, Oral drug absorption enhancement by chitosan and its derivatives, Adv. Drug Deliv. Rev. 52 (2001) 117–126.

[13] K.A. Janes, M.P. Fresneau, A.F. Ana Marazuela, M.J. Alonso, Chitosan nanoparticles as delivery systems for doxorubicin, J. Control Rel. 73 (2001) 255–267.

[14] B. Sarmento, S. Martins, A. Ribeiro, F. Veiga, R. Neufeld, D. Ferreira, Development and comparison of different nanoparticulate polyelectrolyte complexes as insulin carriers, Int. J. Pept. Res. Ther. 12 (2006) 131–138.

[15] N. Kamiya, A.M. Klibanov, Controlling the rate of protein release from polyelectrolyte complexes, Biotechnol. Bioeng. 82 (2003) 590–594.

[16] T. Sakiyama, H. Takata, M. Kikuchi, K. Nakanishi, Polyelectrolyte complex gel with high pH-sensitivity prepared from dextran sulfate and chitosan, J. Appl. Polym. Sci. 73 (1999) 2227–2233.

[17] T. Sakiyama, H. Takata, T. Toga, K. Nakanishi, pH-sensitive shrinking of a dextran sulfate/chitosan complex gel and its promotion effect on the release of polymeric substances, J. Appl. Polym. Sci. 81 (2001) 667–674.

[18] T. Serizawa, M. Yamaguchi, A. Kishida, M. Akashi, Alternating gene expression in fibroblasts adhering to multilayers of chitosan and dextran sulfate, J. Biomed. Mater. Res. 67 (2003) 1060–1063.

[19] A.M. Dyer, M. Hinchcliffe, P. Watts, J. Castile, I. Jabbal-Gill, R. Nankervis, A. Smith, L. Illum, Nasal delivery of insulin using novel chitosan based formulations: a comparative study in two animal models between simple chitosan formulations and chitosan nanoparticles, Pharm. Res. 19 (2002) 998–1008.

[20] C. Lin, R. Gokhale, J.S. Trivedi, V. Ranade, Recent strategies and methods for improving insulin delivery, Drug Dev. Res. 63 (2004) 151–160.

[21] J.S. Patton, J. Bukar, S. Nagarajan, Inhaled insulin, Adv. Drug Deliv. Rev. 35 (1999) 235–247.

[22] A. Fasano, Innovative strategies for the oral delivery of drugs and peptides, Trends Biotechnol. 16 (1998) 152–157.

[23] C. Vauthier, C. Dubernet, E. Fattal, H. Pinto-Alphandary, P. Couvreur, Poly(alkylcyanoacrylates) as biodegradable materials for biomedical applications, Adv. Drug Deliv. Rev. 55 (2003) 519–548.

[24] M.M. Bradford, A rapid and sensitive method for the quantitation of microgram quantities of protein utilizing the principle of protein–dye binding, Anal. Biochem. 72 (1976) 248–254.

[25] A. Dong, P. Huang, W.S. Caughey, Protein secondary structures in water from second-derivative Amide I infrared spectra, Biochemistry 29 (1990) 3303–3308.

[26] B. Sarmento, A. Ribeiro, F. Veiga, D. Ferreira, Development and validation of a rapid reversed-phase HPLC method for the determination of insulin from nanoparticulate systems, Biomed. Chromatogr. 20 (2006) 898–903.

[27] M. van de Weert, W.E. Hennink, W. Jiskoot, Protein instability in poly(lactic-*co*-glycolic acid) microparticles, Pharm. Res. 17 (2000) 1159–1167.

[28] J. Brange, Galenics of Insulin: The Physico-chemical and Pharmaceutical Aspects of Insulin, Insulin Preparations, Springer-Verlag, 1987.

[29] Y. Pan, Y.J. Li, H.Y. Zhao, J.M. Zheng, H. Xu, G. Wei, J.S. Hao, F.D. Cui, Bioadhesive polysaccharide in protein delivery system: chitosan nanoparticles improve the intestinal absorption of insulin in vivo, Int. J. Pharm. 249 (2002) 139–147.

[30] M.J. Zohuriaan, F. Shokrolahi, Thermal studies on natural and modified gums, Polym. Test 23 (2004) 575–579.

[31] B. Sarmento, D. Ferreira, F. Veiga, A. Ribeiro, Characterization of insulin-loaded alginate nanoparticles produced by ionotropic pre-gelation through DSC and FTIR studies, Carbohyd. Polym. 66 (2006) 1–7.

[32] M. Fuentes, B.C.C. Pessela, J.V. Maquiese, C. Ortiz, R.L. Segura, J.M. Palomo, O. Abian, R. Torres, C. Mateo, R. Fernandez-Lafuente, J.M. Guisan, Reversible and strong immobilization of proteins by ionic exchange on supports coated with sulfate-dextran, Biotechnol. Prog. 20 (2004) 1134–1139.

[33] L. Jorgensen, M.v.d. Weert, C. Vermehren, S. Bjerregaard, S. Frokjaer, Probing structural changes of proteins incorporated into water-in-oil emulsions, J. Pharm. Sci. 93 (2004) 1847–1859.

[34] U. Bilati, E. Allémann, E. Doelker, Strategic approaches for overcoming peptide and protein instability within biodegradable nano- and microparticles, Eur. J. Pharm. Biopharm. 59 (2005) 375–388.

[35] G. Kersten, J. Westdijk, in: Wim Jiskoot, D.J.A. Crommelin (Eds.), Methods for Structural Analysis of Protein Pharmaceuticals, AAPS Press, 2005.

[36] L. Nielsen, S. Frokjaer, J. Brange, V.N. Uversky, A.L. Fink, Probing the mechanism of insulin fibril formation with insulin mutants, Biochemistry 40 (2001) 8397–8409.

[37] J. Brange, Stability of Insulin, Kluwer Academic Publishers, 1994.